MALAYSIAN JOURNAL OF SCIENCE
MJS
ISSN 1394-3065

Regular Issue

Malaysian Journal of Science 44 (3): 50-55 (September 2025) https://mjs.um.edu.my

Synthesis and Photocatalytic Performance Evaluation of $BaTiO_3/ZnO/Cs_3Bi_2I_9$ Based Perovskite for Solar Cell Applications

Hala Allawi Kadhim[1a]* and Majida Hameed Khazaal[2a]

Abstract: Due to the light absorption properties of perovskites, including halides, perovskite cells are considered an ideal energy system. This study aims to improve photoexcitation separation by introducing a material with a perovskite-like structure, such as $Cs_3Bi_2I_9$, alone or with barium titanate nanoparticles as a second choice, while the third choice is to impregnate barium titanate (prepared by hydrothermal method) with ZnO to form $BaTiO_3/ZnO$, then mix it with $Cs_3Bi_2I_9$. All these choices are fabricated as a sandwich between the n-type and p-type collection. The produced layers, $BaTiO_3/ZnO/Cs_3Bi_2I_9$, were characterized using XRD, EDX, SEM, and UV-Vis spectroscopic analytical techniques. The results suggest that the band gap of the prepared layer was further decreased compared to the original material, $Cs_3Bi_2I_9$. The performance test revealed a photo conversion efficiency (PCE) of 3.13% and a highest power of 3.15 MW, comparable to or higher than other studies. This suggests that this layer significantly reduces recombination phenomena and improves the cell's performance overall.

Keywords: *Perovskites, solar cells, nanoparticles, thermal method, barium titanate.*

1. Introduction

The availability of energy sources determines how quickly the global economy grows. All energy conversions impact the environment (Hamed & Alshare, 2022). For example, the widespread use of fossil fuels in almost all human endeavors has led to unfavorable events, including air and environmental pollution. Consequently, terms related to global warming, climate change, and ozone depletion appeared more often in the literature (Gunerhan et al., 2009). Since solar energy is among the planet's most significant renewable energy sources and is thought to be the primary force behind economic growth, researchers have worked to replace fossil fuels with solar energy that is clean, renewable, and environmentally friendly. Solar energy is the most abundant renewable energy source since it is readily available compared to other energy sources such as wind, geothermal, hydropower, wave, and tidal. (Pescoe & Ali, n.d.). In recent decades, prior studies have been conducted on optoelectronic conversion, a primary application of solar energy. Solar cells are the most important type of optoelectronic converter. Developing low-cost, highly efficient solar cells has recently become the primary focus. Perovskite solar cells (PSCs) have received significant attention in the past decade because they have outstanding bipolar charge mobility, a long carrier diffusion length, a low trap state density, a changeable bandgap, and a high absorption coefficient. These characteristics make them a promising class of solar cells (Wang et al., 2021). The perovskite consists of an organic-inorganic hybrid material (OIHP) with a structure described by the formula ABX_3. In this formula, X represents a halogen ion, B represents a divalent ion, and A represents a monovalent ion. These materials have become prominent due to their exceptional optical and electrical properties, as well as their simplicity and cost (H. Tanaka et al., 2018). Within ten years, PSCs' photoelectric conversion proficiency (PCE) climbed from approximately 3% to 25% (C. Zhang et al., 2022). As a result of their simple construction method and optimal conversion efficiency, $CH_3NH_3PbI_3$-based perovskite for solar cells has been the focus of recent research. However, due to its toxicity and the fact that it contains Pb as a heavy element (Tomaszewski, 1994), researchers attempted to replace it with Sn and Ge, which can substitute Pb to form a less toxic perovskite structure. However, in the air presence, Sn^{2+} and Ge2+ exhibit less stability than Pb^{2+} and can easily oxidize into Sn^{4+} and Ge^{4+}. These higher oxidation states are more persistent in an oxidizing atmosphere, leading to the swift destruction of the perovskite structure.

Consequently, Bi-based halide perovskites with the formulation $A_3Bi_2X_9$ (A represents a monovalent cation, such as Na^+, K^+, Rb^+, or Cs^+) have gained attention due to their capacity to address the stability and toxicity concerns associated with lead-based materials (Bai et al., 2018). In several studies (Park et al., 2015; Zhang et al., 2017; [8]), scientists report achieving power conversion efficiency of 1.09%, 1.64%, and 2.3%. To improve conversion efficiency, it is crucial to implement modifications in the working method, incorporate additional materials, reduce the energy gap, expand the depletion region, augment the quantity of charge carriers, and avoid recombination (K. Tanaka et al., 2003). Research on ceramic materials with high dielectric

Authors information:
[a]Chemistry, University of Kufa, AlKufa, IRAQ. E-mail: halaa.altaai@student.uokufa.edu.iq[1]; majidah.alkhazaali@uokufa.edu.iq[2]
*Corresponding Author: halaa.altaai@student.uokufa.edu.iq

Received: June, 2023
Accepted: June, 2024
Published: June, 2025

DOI: https//doi.org/10.22452/mjs.vol44no3.5
Malaysian Journal of Science 44(3): 50-55 (June 2025)

constants, like $BaTiO_3$, has increased in recent years due to these variables and their related influences. Simultaneously, the significance of ceramics is increasing due to the rapid advancement of electromagnetic technologies, which elevates the dielectric constant of particles.

Researchers have extensively studied $BaTiO_3$, a dielectric material, mainly due to its increased dielectric constant, minimal dielectric loss, and substantial dielectric coefficient, all of which contribute to a strong electric field (Maison et al., 2003), (Sengupta et al., 1995). Nanotechnology is rapidly progressing in various domains, particularly solar cells, where scientists have successfully integrated nanoparticles to enhance the cells' energy transfer efficiency and discover sustainable energy alternatives. Scientists design nanoparticles to reduce static electricity from the polar surface's pre-existing ionic charge (Rabiei et al., 2020). Barium titanate (BaTiO3) is an electrical insulator, a ferroelectric ceramic substance. Nevertheless, it behaves like a semiconductor when doped with trace amounts of metals, such as scandium, yttrium, neodymium, cesium, etc. (Ray, 2007). The PSCs are filled with ferroelectric materials, which eventually regulate the residual polarization electric field by altering it through the external electric field, thereby controlling the carrier and ion transport [6]. The researchers synthesized several zinc oxide nanostructures and observed that zinc oxide enhances light harvesting, electron and energy transfer, and cell conversion efficiency. This is achieved by establishing a unidirectional pathway for rapid electron transmission within the layers of the photoanode (Omar & Abdullah, 2014).

In this work, inorganic nanomaterials, $BaTiO_3$ and $BaTiO_3$/ZnO, were synthesized and combined with $Cs_3Bi_2I_9$ to form the anode electrode for the cell. The perovskite layer exhibited robust spontaneous polarization characteristics, as evidenced by these materials. The synthesized material was subjected to characterization techniques such as optical properties, XRD, SEM, UV, and EDS to gain insights into its properties.

2. Experimental

Preparation of Compounds

All salts and solvents ($Ba(OH)_2$. $8H_2O$, 99%), (BiI_3, 99%), (CsI, 99.9%), ammonia solution (10 M), anhydrous N, N-dimethylformamide (DMF, 99.8%), titanium dioxide, acetylacetonate, CH_3OH (anhydrous, 99.8%), dimethylsulfide (DMSO) and $Zn\{NO_3\}_2$ utilized in the synthesis procedures were acquired from Alpha Chemika-India and used without any additional purification treatments. Preparations of $BaTiO_3$, ZnO, $Cs3Bi2I_9$, and nano copper oxide were prepared according to (Park et al., 2015), (C. Zhang et al., 2022), (Viewcontent.Cgi, n.d.), (Al-Marzouki et al., 2011).

After preparation in above, $BaTiO_3$/ZnO, was prepared by the impregnation method in a ration of 2g of $BaTiO_3$ to 1 g of $Zn\{NO3)_2$ for about 24h at 30^{0}C, after that drying at 75^{0}C for 30 minutes, then it was calcined in the oven at 300^{0}C for 2h. $Cs_3Bi_2I_9$ solution was prepared by dissolving a mixture of BiI_3 (1.65 M) and CsI (2.475 M) in 50 ml of DMF and stirring for 24 h at 70 °C. Some details of the preparation steps are shown in Scheme 1.

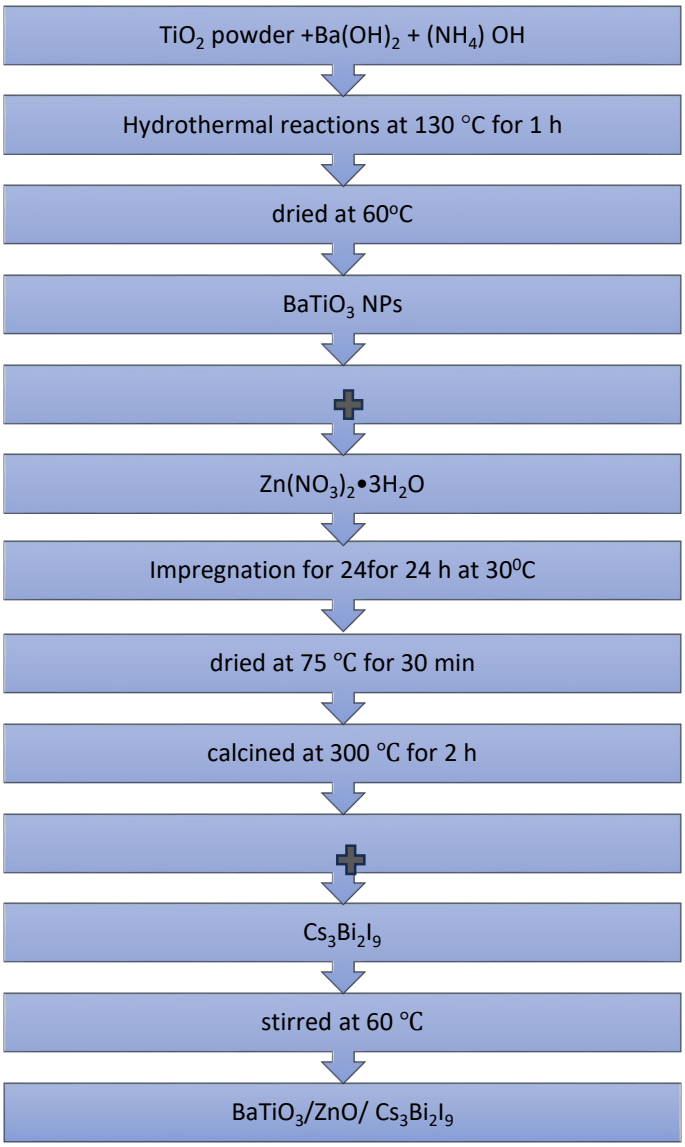

Scheme 1. Preparation steps of (1) $BaTiO_3$, (2) $BaTiO_3$/ZnO, (3) $BaTiO_3$/ZnO /$Cs_3Bi_2I_9$.

Fabrication of Devices

Cleaning of the Indium tin oxide (ITO) glass with alcohol is the initial step. A layer of TiO_2 was prepared by mixing ethyl alcohol with TiO_2 in a ratio of 1:7 via drip-coated (ETM) precursor. The TiO_2 precursor was treated for 30 minutes at 500 ^{0}C. This layer was coated with a second layer by dripping of either of the following:

1. Solution of $Cs_3Bi_2I_9$
2. mixture of $BaTiO_3$/$Cs_3Bi_2I_9$, and
3. Mixture of $BaTiO_3$/ZnO/$Cs_3Bi_2I_9$

It is worth noting that mixtures of 2 and 3 are obtained by adding some drops of Cs3Bi2I9 to BaTiO3 and BaTiO3/ZnO. A 5 mL chlorobenzene was added to each one to prevent agglomeration.

Next, an annealing treatment was carried out for the prepared layers in two stages on the heating platform (60 ^{0}C for two minutes and 120 ^{0}C for ten minutes). In order to create the p-type HTM composite by drop coating, 3 mg of CuO nanocompound and 1 ml of chlorobenzene were mixed. Aluminum foil of (1 cm x 1 cm)

DOI: https//doi.org/10.22452/mjs.vol44no3.5
Malaysian Journal of Science 44(3): 50-55 (June 2025)

was pressed as a counter electrode. The whole assembly is shown in Figure 1.

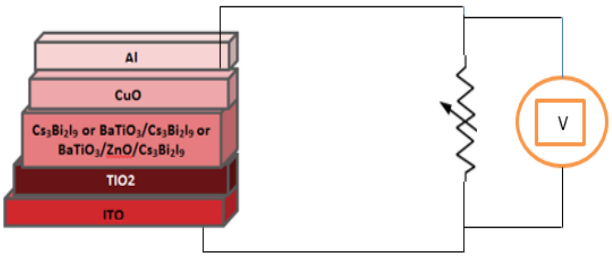

Figure 1. Assembly of the device with I-V measurement circuit

3. Characterization Analysis

X-ray diffraction (XRD, model -6000 Shimadzu, Japan) was employed to estimate the size and crystal structure of the sample using Cu Kα radiation (μ = 1.5406 Å). The surface morphologies and elemental analysis were characterized using a scanning electron microscope (SEM) of the type VEGA 3SBU-NO118-0014 with Energy-dispersive X-ray spectroscopy EDS. The band gap of the materials was determined using UV-1800 SHIMADZU spectroscopy. 1 cm^2 was identified as the effective area of the cell, using the variable resistance box (type 8000-England) and digital multimeter (FLUKE 17B), the J-V curves of the prepared PSCs were measured (Figure 1).

4. Result and Discussion

X-ray diffraction analysis is used to determine the crystallinity and particle size of nanomaterials using the Scherrer equation, which has the following form:

$$L=\frac{k\lambda}{BCos\theta}, \quad (1)$$

where K is a constant and L is the nano crystal size (Harbbi & Jahil, 2017). As per a prior work (Rabiei et al., 2020), ε represents the wavelength of radiation in nanometers (λ Cu Kα = 0.15405 nm); θ denotes the diffracted angle of the peak; and β signifies the total width of the peak at half maximum in radians. Figure (2) shows the synthetic compounds' XRD pattern. All the peaks shown in Figure 2a are related to the BaTiO3 phase. According to Scherrer's equation, equation 1, the $BaTiO_3$ crystallite size average was 55.85 nm. Nevertheless, the outcomes demonstrated that the size shifted to 25–68 nm after interacting with ZnO and $Cs_3Bi_2I_9$. The hexagonal $Cs_3Bi_2I_9$ perovskite structure (space group of P63/mmc (194); a=8.40, b=8.40, and c=21.25 Å) was well-represented in the crystalline phase of all the $Cs_3Bi_2I_9$ films. Figure 2b indicates that a high crystallinity perovskite phase occurred in these films, as confirmed by firm peaks at 2θ = 12.85° and 26.80°. All of the observed peaks show displacement after the mixing procedure, with the angle shift rising for larger two θ (Figure 2c) (Zou2012.Pdf, n.d.).This implies that the cation changes inside the perovskite structure have some effect on the structure. X-ray diffraction figure (2d) illustrates the nanoscale of the copper oxide crystal and the absence of any other peaks, indicating the compound's purity and lack of impurities.

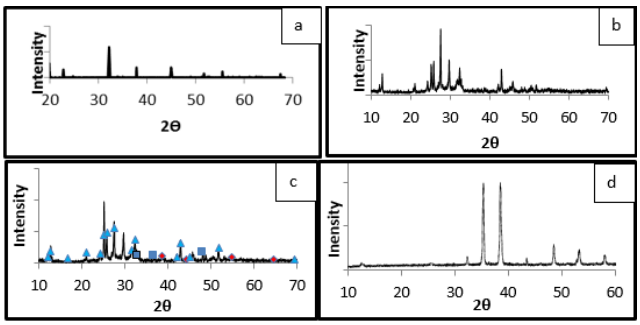

Figure 2. XRD patterns of (a) $Cs_3Bi_2I_9$ (b) $BaTiO_3$ (c) $BaTiO_3$/ZnO/ $Cs_3Bi_2I_9$ (d) CuO powder

The elemental elements of the perovskite components were analyzed using the EDS technique. The results are shown in Figure 3.

DOI: https//doi.org/10.22452/mjs.vol44no3.5
Malaysian Journal of Science 44(3): 50-55 (June 2025)

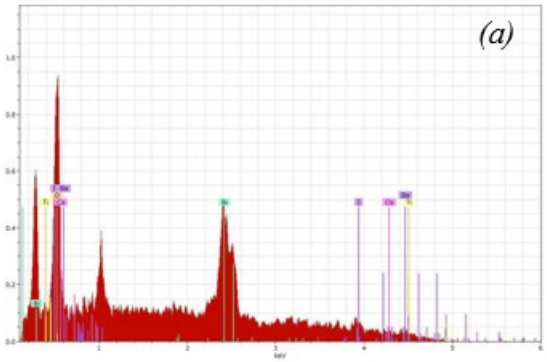

El	AN	Series	unn. C [wt.%]	norm. C [wt.%]	Atom. C [at.%]	Error (1 Sigma) [wt.%]
Bi	83	M-series	43.48	46.05	18.26	3.10
Cs	55	M-series	26.02	27.56	17.18	19.10
O	8	K-series	8.17	8.66	44.85	2.12
Ti	22	L-series	7.22	7.65	13.24	3.29
I	53	M-series	7.04	7.46	4.87	3.79
Ba	56	M-series	2.48	2.62	1.58	2.17
Total:			94.41	100.00	100.00	

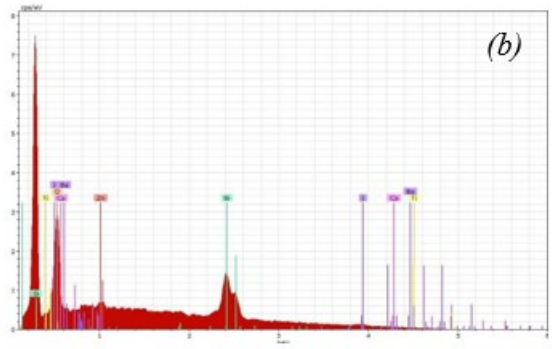

El	AN	Series	unn. C [wt.%]	norm. C [wt.%]	Atom. C [at.%]	Error (1 Sigma) [wt.%]
Bi	83	M-series	31.47	41.70	16.31	2.37
Cs	55	M-series	14.82	19.64	12.08	14.23
I	53	M-series	13.83	18.32	11.80	5.79
O	8	K-series	6.39	8.47	43.28	1.82
Ti	22	L-series	6.31	8.36	14.26	3.06
Ba	56	M-series	2.43	3.22	1.92	2.19
Zn	30	L-series	0.22	0.29	0.36	0.10
Total:			75.46	100.00	100.00	

Figure 3. EDS analysis for (a) $BaTiO_3$/ $Cs_3Bi_2I_9$ (b) $BaTiO_3$/ZnO/ $Cs_3Bi_2I_9$

The optical properties of the produced compounds ($Cs_3Bi_2I_9$, $BaTiO_3$, $BaTiO_3/Cs_3Bi_2I_9$, and $BaTiO_3/ZnO/Cs_3Bi_2I_9$) were measured. It was found that these compounds absorb light in the uv-visible range, as shown in Figure 4, where a significant change in the absorbance peak from 300 nm for $BaTiO_3$ (Figure 4b) to 500 nm for $BaTiO_3/Cs_3Bi_2I_9$ and 600 nm for $BaTiO_3/ZnO/Cs_3Bi_2I_9$ as shown in Figures (4c and 4d). Cs3Bi2I9, on the other hand, absorbs light at 400 nm (Figure 4a), and its energy band gap is 3.1 ev (Figure 4e). The energy band gap shifted, as calculated by the Tauc relationship (Mehta et al., 2009) in Equation (2), changed from 3.8(ev) for $BaTiO_3$ figure (4f) to 2.8(ev) for $BaTiO_3/Cs_3Bi_2I_9$ (Figure 4g).

$$\propto \lambda V) = C(hv - Eg)^n \qquad (2)$$

for $BaTiO_3/ZnO/Cs_3Bi_2I_9$ and 2.4 (ev) (Figure 4h), where $\propto$ is the absorption coefficient, C is a constant, Eg is the band gap of the molecule, and n varies based on the type of transition. The linear portion of the $(\alpha\lambda v)^2$ vs.hv intercept was used to compute the usual band gap.

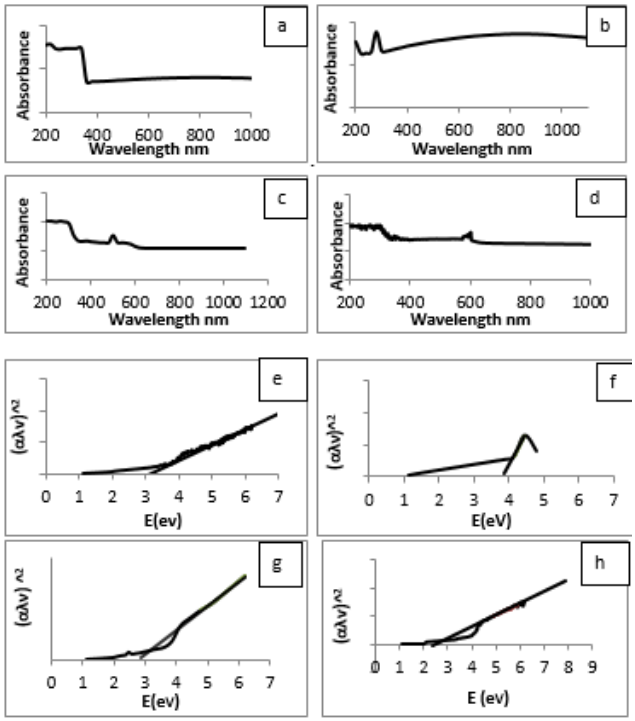

Figure 4. UV-Vis spectra of (a) $Cs_3Bi_2I_9$ (b) $BaTiO_3$ (c) $BaTiO_3/Cs_3Bi_2I_9$, (d) $BaTiO_3/ZnO/Cs_3Bi_2I_9$. The band gap of (e) $Cs_3Bi_2I_9$, (f) $BaTiO_3$ (g) $Cs_3Bi_2I_9/BaTiO_3$ (h) $BaTiO_3/ZnO/Cs_3Bi_2I_9$

DOI: https//doi.org/10.22452/mjs.vol44no3.5
Malaysian Journal of Science 44(3): 50-55 (June 2025)

The scanning electron microscope (SEM) shows that the morphology of barium titanate produced by the hydrothermal process is very different from that of barium titanate combined with perovskite (Figure 5a), where the surface of BaTiO3 has large grains with the appearance of clear voids, high surface area and excellent electrode porosity are the desirable criteria for a high efficiency. $Cs_3Bi_2I_9/BaTiO_3$ figure (5b) may have a higher perovskite adsorption due to its increased porosity. When zinc oxide (5c) is added, the surface seems more regular and takes on a more uniform shape, as shown in Figure 5d.

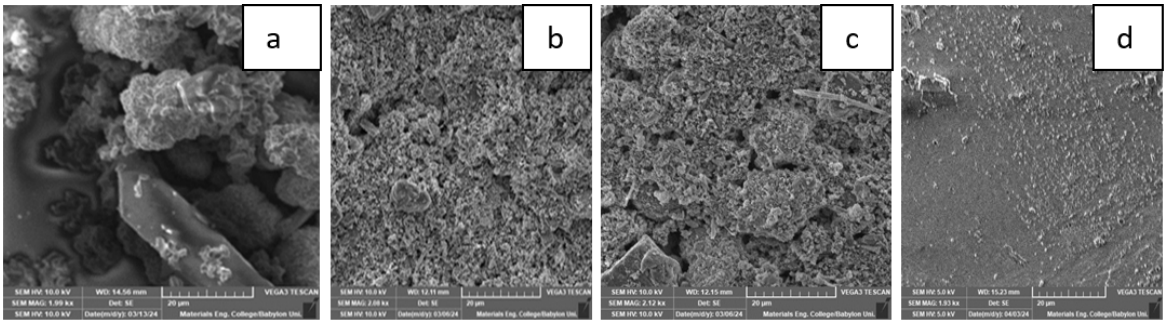

Figure 5. SEM of the surface (a) $BaTiO_3$ (b) $Cs_3Bi_2I_9$ /$BaTiO_3$ (c) $BaTiO_3$/ZnO (d) $BaTiO_3$/ZnO/ $Cs_3Bi_2I_9$.

The modified perovskite $BaTiO_3$/ZnO/ $Cs_3Bi_2I_9$ has the highest current compared to standard perovskite $Cs_3Bi_2I_9$. As a result, a modified perovskite $BaTiO_3$/ $Cs_3Bi_2I_9$ has the highest efficiency, reaching 3.13% (which is better according to a prior study (Park et al., 2015)), with a short-circuit current of 6.16 mA and an open-circuit voltage of 0.73V. According to the current-voltage (I-V) curve, the highest power is 3.15mw, as shown in Figure 6. The photovoltaic parameters are abstracted, as shown in Table 1.

For the Cs3Bi2I9 compound, photo-electric conversion efficiency is the lowest amongst other compounds, which is attributed to the ease of recombination effect. This efficiency is improved significantly by the addition of barium titanate. The efficiency reaches about 2.4% due to the polarization field effect on the piezoelectric materials, which affects the photocatalytic properties. In the piezoelectric effect, the separation of the electron-hole pair is promoted due to the incident photon. The role of BaTiO3 is to enhance the separation of electron-hole pairs by spontaneous polarization, which is apparent in the efficiency values (see Table 1).

With the addition of BaTiO3/ZnO to Cs3Bi2I9, the efficiency reaches 4.17%, representing an enhanced value compared to $Cs_3Bi_2I_9$/ $BaTiO_3$. This efficiency enhancement can be explained by considering the small particle size, smooth surface features, the highest absorption, and the low value of ZnO band gap.

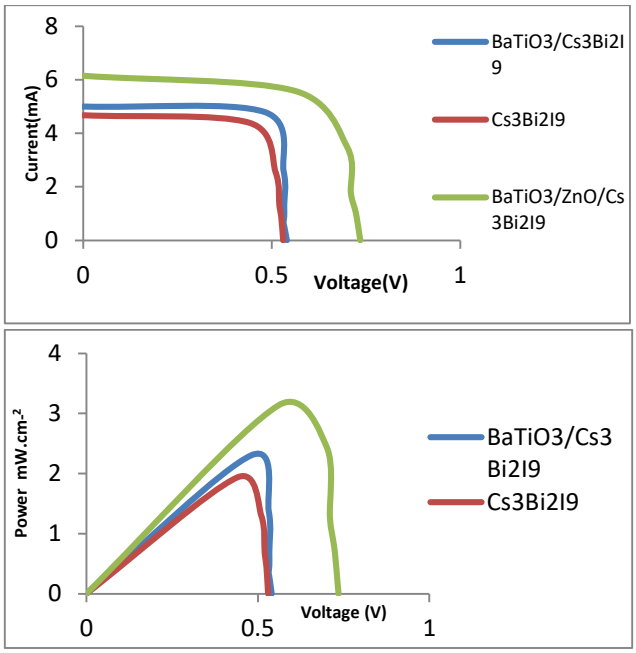

Figure 6. (a) I-V (b) power-V characteristic for $Cs_3Bi_2I_9$, $Cs_3Bi_2I_9$/ $BaTiO_3$, $BaTiO_3$/ZnO/ $Cs_3Bi_2I_9$ for active area 1 cm^2 under light intensity (100 mw/cm^2).

Table 1. Photoelectrical parameters of $Cs_3Bi_2I_9$, $Cs_3Bi_2I_9$/ $BaTiO_3$, $BaTiO_3$/ZnO/ $Cs_3Bi_2I_9$ for active area 1 cm^2 under light intensity (100 mw/cm^2)

MIX	V_{oc} *v*	I_{sc} *mA*	*FF*	η *%*
$Cs_3Bi_2I_9$	0.53	4.68	0.78	1.93
$Cs_3Bi_2I_9$ /$BaTiO_3$	0.54	5	0.85	2.4
$BaTiO_3$/ZnO/ $Cs_3Bi_2I_9$	0.73	6.16	0.87	3.13

DOI: https//doi.org/10.22452/mjs.vol44no3.5
Malaysian Journal of Science 44(3): 50-55 (June 2025)

5. Conclusion

In this work, barium titanate was impregnated with zinc oxide nanoparticles. tt was then mixed with perovskite to yield $BaTiO_3/ZnO/Cs_3Bi_2I_9$ as a product, which yielded an improved efficiency of 3.13% and 3.15 mw. An open circuit voltage of 0.73 V was also detected. Improving the efficiency is due to the ease of extracting carriers where the charge is transferred through the perovskite layer and modified with zinc oxide. The lack of recombination of the charge carriers is also due to the compound having the highest absorption value and the lowest energy band gap.

5. References

Bai, F., Hu, Y., Hu, Y., Qiu, T., Miao, X., & Zhang, S. (2018). he first and cost effectivenano-biocomposite, zinc porphyrin/ CuO/reduced graphene oxide, based on Calotropis procera plant for perovskite solar cellas hole. *Solar Energy Materials and Solar Cells*, *184*(January), 15–21. https://doi.org/10.1016/j.solmat.2018.04.032

Gunerhan, H., Hepbasli, A., & Giresunlu, U. (2009). Environmental impacts from the solar energy systems. *Energy Sources, Part A: Recovery, Utilization and Environmental Effects*, *31*(2), 1131–1138. https://doi.org/10.1080/15567030701512733

Hamed, T. A., & Alshare, A. (2022). Environmental Impact of Solar and Wind energy-A Review. *Journal of Sustainable Development of Energy, Water and Environment Systems*, *10*(2), 1–23. https://doi.org/10.13044/j.sdewes.d9.0387

Harbbi, K. H., & Jahil, S. S. (2017). Study the Lattice Distortion and Particle Size of One Phase of MnO by Using Fourier Analysis of X-ray Diffraction Lines. *Advances in Physics Theories and Applications*, *65*(x), 6–22.

Maison, W., Kleeberg, R., Heimann, R. B., & Phanichphant, S. (2003). Phase content, tetragonality, and crystallite size of nanoscaled barium titanate synthesized by the catecholate process: Effect of calcination temperature. *Journal of the European Ceramic Society*, *23*(1), 127–132. https://doi.org/10.1016/S0955-2219(02)00071-7

Mehta, S. K., Kumar, S., Chaudhary, S., & Bhasin, K. K. (2009). Supplementary Material (ESI) for Nanoscale Supplementary data Nucleation and growth of surfactant passivated CdS and HgS NPs: Time dependent Absorption and Luminescence profiles. *The Royal Society of Chemistry*, *c*, 1–6.

Omar, A., & Abdullah, H. (2014). Electron transport analysis in zinc oxide-based dye-sensitized solar cells: A review. *Renewable and Sustainable Energy Reviews*, *31*, 149–157. https://doi.org/10.1016/j.rser.2013.11.031

Park, B. W., Philippe, B., Zhang, X., Rensmo, H., Boschloo, G., & Johansson, E. M. J. (2015). B. W. Park, B. Philippe. *Advanced Materials*, *27*(43), 6806–6813. https://doi.org/10.1002/adma.201501978

Pescoe, ©, & Ali, F. M. (n.d.). *A Review on Solar Energy Potential And Future world*.

Rabiei, M., Palevicius, A., Monshi, A., Nasiri, S., Vilkauskas, A., & Janusas, G. (2020). Comparing methods for calculating nano crystal size of natural hydroxyapatite using X-ray diffraction. *Nanomaterials*, *10*(9), 1–21. https://doi.org/10.3390/nano10091627

Ray, A. K. (2007). *SYNTHESIS AND CHARACTERIZATION OF BaTiO3 POWDER PREPARED BY COMBUSTION SYNTHESIS PROCESS SYNTHESIS AND CHARACTERIZATION OF BaTiO3 POWDER PREPARED BY COMBUSTION SYNTHESIS PROCESS*.

Sengupta, L. C., Stowell, S., Ngo, E., Oday, M. E., & Lancto, R. (1995). Barium strontium titanate and nonferroelectric oxide ceramic composites for use in phased array antennas. *Integrated Ferroelectrics*, *8*(1–2), 77–88. https://doi.org/10.1080/10584589508012302

Tanaka, H., Oku, T., & Ueoka, N. (2018). Structural stabilities of organic–inorganic perovskite crystals. *Japanese Journal of Applied Physics*, *57*(8), 0–9. https://doi.org/10.7567/JJAP.57.08RE12

Tanaka, K., Takahashi, T., Ban, T., Kondo, T., Uchida, K., & Miura, N. (2003). Comparative study on the excitons in lead-halide-based perovskite-type crystals CH3NH3PbBr3 CH3NH 3PbI3. *Solid State Communications*, *127*(9–10), 619–623. https://doi.org/10.1016/S0038-1098(03)00566-0

Tomaszewski, P. E. (1994). Crystal Structure and Phase Transitions in the A3B2X9 Family of Crystals. *Physica Status Solidi (B)*, *181*(1), 15–21. https://doi.org/10.1002/pssb.2221810102

Wang, M., Wang, W., Ma, B., Shen, W., Liu, L., Cao, K., Chen, S., & Huang, W. (2021). Lead-Free Perovskite Materials for Solar Cells. In *Nano-Micro Letters* (Vol. 13, Issue 1). Springer Singapore. https://doi.org/10.1007/s40820-020-00578-z

Zhang, C., Li, X., Ding, L., Jin, C., & Tao, H. (2022). Effect of BaTiO3 powder as an additive in perovskite films on solar cells. *RSC Advances*, *12*(13), 7950–7960. https://doi.org/10.1039/d1ra09374f

Zhang, Z., Li, X., Xia, X., Wang, Z., Huang, Z., Lei, B., & Gao, Y. (2017). High-Quality (CH3NH3)3Bi2I9 Film-Based Solar Cells: Pushing Efficiency up to 1.64%. *Journal of Physical Chemistry Letters*, *8*(17), 4300–4307. https://doi.org/10.1021/acs.jpclett.7b01952*zou2012.pdf*. (n.d.).

DOI: https//doi.org/10.22452/mjs.vol44no3.5
Malaysian Journal of Science 44(3): 50-55 (June 2025)